

## SDSS J143030.22–001115.1: A Misclassified Narrow-line Seyfert 1 Galaxy with Flat X-ray Spectrum \*

Wei-Hao Bian<sup>1,2</sup>, Quan-Ling Cui<sup>1</sup> and Li-Hua Chao<sup>1</sup>

<sup>1</sup> Department of Physics and Institute of Theoretical Physics, Nanjing Normal University, Nanjing 210097 [whbian@njnu.edu.cn](mailto:whbian@njnu.edu.cn)

<sup>2</sup> Key Laboratory for Particle Astrophysics, Institute of High Energy Physics, Chinese Academy of Sciences, Beijing 100049

Received 2005 October 8; accepted 2006 January 6

**Abstract** We used multi-component profiles to model the  $H\beta$  and  $[O\ III]\lambda\lambda 4959, 5007$  lines of SDSS J143030.22–001115.1, a narrow-line Seyfert 1 galaxy (NLS1) in a sample of 150 NLS1 candidates selected from the Sloan Digital Sky Survey (SDSS), Early Data Release (EDR). After subtracting the  $H\beta$  contribution from narrow line regions (NLRs), we found that its full width half maximum (FWHM) of broad  $H\beta$  line is nearly  $2900\text{ km s}^{-1}$ , significantly larger than the customarily adopted criterion of  $2000\text{ km s}^{-1}$ . With its weak Fe II multiples, we believe that SDSS J143030.22–001115.1 should not be classified as a genuine NLS1. When we calculate the virial black hole masses of NLS1s, we should use the  $H\beta$  linewidth after subtracting the NLR component.

**Key words:** galaxies: active — galaxies: emission lines — galaxies: nuclei — galaxies: Seyfert — galaxies: individual: J143030.22–001115.1

### 1 INTRODUCTION

Narrow-line Seyfert 1 galaxies (NLS1s) were defined by their optical spectral characteristics:  $H\beta$  full width half maximum (FWHM) less than  $2000\text{ km s}^{-1}$ , strong optical Fe II multiples, and the line-intensity ratio of  $[O\ III]\lambda 5007$  to  $H\beta$  less than 3 (Osterbrock & Pogge 1985; Goodrich 1998). These properties suggest that NLS1s likely contain less massive black holes with higher Eddington ratios (Pounds et al. 1995; Wandel & Boller 1998; Laor et al. 1997; Mineshige et al. 2000), putting NLS1s at one extreme end of the so-called Boroson & Green (1992) eigenvector 1. Their locus in the  $M - \sigma$  relation plane is possibly special in relation to the other AGNs (e.g., Bian & Zhao 2004; Grupe & Mathur 2004; Greene & Ho 2006). X-ray observations of NLS1s have revealed a strong X-ray excess, and NLS1s generally have softer X-ray spectra than other AGNs (Boller et al. 1996; Leighly 1999). Grupe et al. (2004) found that selection by ultra-soft X-ray can lead to finding large numbers of NLS1s.

Williams et al. (2003) presented a sample of 150 NLS1 candidates found in the Sloan Digital Sky Survey (SDSS) Early Data Release (EDR) (Stoughton et al. 2002), which is the largest published dataset of NLS1s<sup>1</sup>; 17 of these have been observed by Chandra and it is suggested that ultrasoft X-ray emission is not

---

\* Supported by the National Natural Science Foundation of China.

<sup>1</sup> Zhou et al. (2006) presented a new sample comprising 2000 NLS1s from SDSS Data Release 3 (DR3).

a universal characteristic of NLS1s (Williams et al. 2004). For two objects with the smallest photon indices, SDSS J125943.59+010255.1 and SDSS J143030.22–001115.1, the photon indices are less than one. For the sample of 150 SDSS NLS1s, we have used multi-component profiles model to analyse carefully the narrow line region (NLR) outflows relative to the broad line regions (BLRs) (Bian, Yuan & Zhao 2005). The largest line-intensity ratio of [O III] $\lambda$ 5007 to narrow H $\beta$  at 9.6 is found in SDSS J143030.22–001115.1.

In this paper, we present our multi-component profile modelling of SDSS J143030.22–001115.1. The spectral analysis method is introduced in Section 2. The results of profile fitting are given in Section 3. Our discussion is presented in the last section. All of the cosmological calculations in this paper assume  $H_0 = 75 \text{ km s}^{-1} \text{ Mpc}^{-1}$ ,  $\Omega_M = 0.3$ , and  $\Omega_\Lambda = 0.7$ .

## 2 DATA AND ANALYSIS

Using the SDSS Query Tool, Williams et al. (2003) selected objects from SDSS EDR that were flagged as QSOs and showed narrow H $\beta$  lines. They then measured the the FWHMs of the H $\beta$  lines and obtained a sample of 150 SDSS NLS1s. SDSS J143030.22–001115.1 is one of the objects in this sample and its spectrum is obtained from SDSS Data Release 3 (DR3; Abazajian et al. 2005) (see the left panel in Fig. 1).

There generally exist strong Fe II multiples in NLS1 optical spectra and also asymmetry in the [O III] and/or H $\beta$  lines. Therefore, we reduced the spectrum of SDSS J143030.22–001115.1 with the multi-component fitting task SPECIFY (Kriss 1994) in the IRAF-STS package. The following were used: (1) the Galactic interstellar reddening curve; (2) Fe II template; (3) power-law continuum; (4) three sets of two-gaussian profiles for the [O III] $\lambda\lambda$ 4959, 5007 and H $\beta$  lines. We take the same linewidth for each component, and fix the flux ratio of [O III] $\lambda$ 4959 to [O III] $\lambda$ 5007 at 1:3. To begin, we did not consider starlight contribution because there were no obvious stellar lines (Gu et al. 2006). For more detail, please refer to Bian, Yuan & Zhao (2005, 2006).

## 3 RESULTS

For SDSS J143030.22–001115.1, the [O III] $\lambda$ 5007 is very strong relative to H $\beta$ , and the Fe II multiples are not too strong (see Fig. 1). The flux ratio of Fe II (between 4434 and 4684 Å) to total H $\beta$  (Fe II  $\lambda$  4570/H $\beta$ ) is  $0.59 \pm 0.17$ , which is much smaller than the mean value for the sample of 150 NLS1s (see fig. 2 in Bian, Yuan & Zhao 2005).

In the left panel of Figure 2, we show two-component fittings of H $\beta$  and [O III] $\lambda\lambda$  4959, 5007 in the rest-frame spectrum of SDSS J143030.22–001115.1. The FWHM and flux of each components are listed in Table 1.

From the left panel of Figure 2 and Table 1, we found that the line-intensity ratio of [O III] $\lambda$ 5007 to the narrow H $\beta$  is  $9.6 \pm 3.8$ , which is consistent with the universal adopted value of 10 from the photoionization model of NLRs clouds. Considering the errors in the linewidth, the FWHM of the narrow H $\beta$  line is consistent with that of the narrow and broad [O III] lines. The FWHM of the broad H $\beta$  line is  $2785 \pm 276 \text{ km s}^{-1}$ .

It is usual to use template built from [O III] or [S II] when modelling narrow H $\beta$  and H $\alpha$  lines (Grupe et al. 1998; Grupe et al. 1999; Grupe et al. 2004; Greene & Ho 2005a, b). Since we used two-component profiles to model the asymmetric [O III] $\lambda$ 5007, we should use three-component profiles to model H $\beta$ , with two components for the NLRs and one for the BLRs. We take the same linewidth for each of the NLR components of H $\beta$  and [O III], with the flux ratio of [O III] to H $\beta$  from NLRs set floating. In the right panel of Figure 2 we show the three-component fit of the H $\beta$  line. The FWHM and flux of each of the components are also listed in Table 2. The line-intensity ratio of [O III] $\lambda$ 5007 to the narrow H $\beta$  line is  $8.2 \pm 3.2$  and the FWHM of the broad H $\beta$  line is  $2911 \pm 210 \text{ km s}^{-1}$ . Therefore, SDSS J143030.22–001115.1 is not a genuine NLS1 when we have subtracted the H $\beta$  contribution from the NLRs.

## 4 DISCUSSION

### 4.1 Black Hole Mass Correction

NLS1s belong to Seyfert 1 galaxies and were initially defined by their optical characteristics: FWHM (H $\beta$ ) less than  $2000 \text{ km s}^{-1}$ , which is usually used to calculate the central black hole virial mass (e.g., Wang

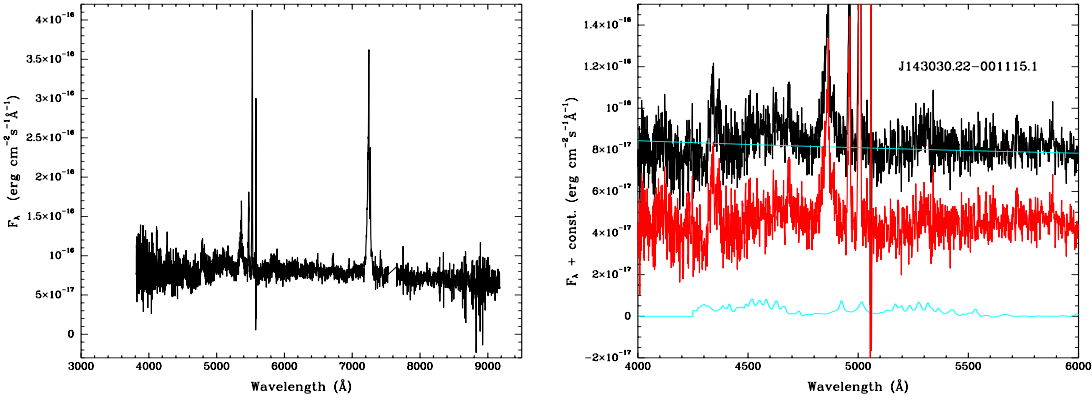


**Fig. 1** Unprocessed spectrum of SDSS J143030.22-001115.1 (left). Rest-frame spectra of SDSS J143030.22-001115.1 (right): the observed spectrum and a power-law continuum (top curve), the Fe II-subtracted spectrum (middle curve), and the Fe II spectrum (bottom curve).

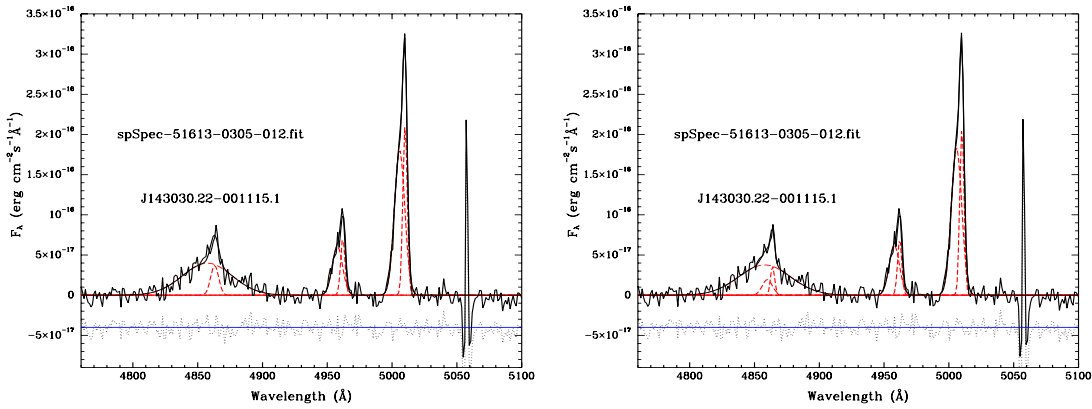


**Fig. 2** Multi-component fittings of the  $H\beta$  and  $[O III]\lambda\lambda 4959, 5007$  lines: the modelled composite profile (thick solid line), the individual components (the dotted lines), and the residual spectrum (lower panel). Left: two-component fit to the  $H\beta$  line; Right: three-component fit to the  $H\beta$  line.

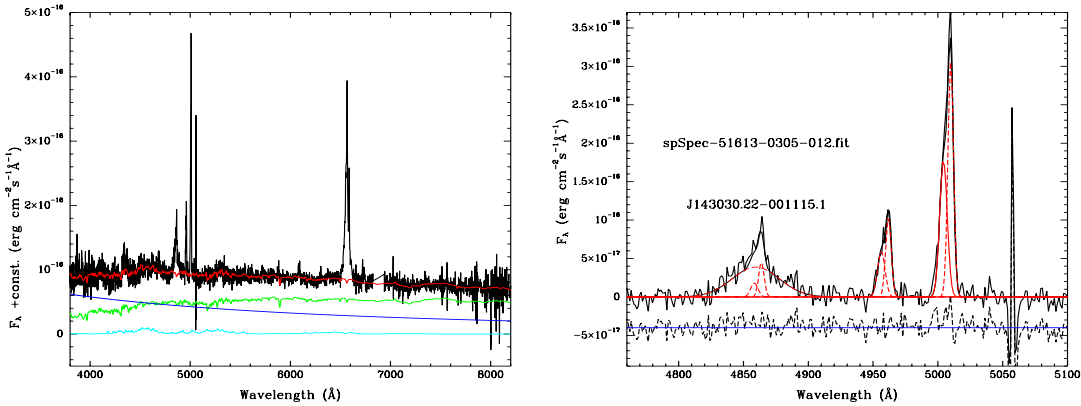


**Fig. 3** Left: the observed spectrum (black curve), a power-law continuum (middle blue curve), Fe II spectrum (bottom cyan curve), starlight contribution (middle Green curve), and combination of the continuum, Fe II and starlight (red curve). Right: three-component fit to the  $H\beta$  line.

**Table 1** Results of the Multi-component Profile Fitting of SDSS J143030.22–001115.1

Line	Component	Rest Wavelength (Å)	FWHM (km s <sup>-1</sup> )	Line flux (10 <sup>-16</sup> erg s <sup>-1</sup> cm <sup>-2</sup> )
(1)	(2)	(3)	(4)	(5)
(Two components to model the H $\beta$ line)				
H $\beta$	n	4859.9 $\pm$ 1.1	447 $\pm$ 199	2.8 $\pm$ 1.1
	b	4854.3 $\pm$ 1.1	2785 $\pm$ 276	19.1 $\pm$ 1.2
[O III] $\lambda$ 4959	n	4960.6 $\pm$ 0.1	238 $\pm$ 21	3.0 $\pm$ 0.5
	b	4956.5 $\pm$ 0.4	563 $\pm$ 27	6.0 $\pm$ 0.5
[O III] $\lambda$ 5007	n	5006.8 $\pm$ 0.1	238 $\pm$ 21	9.0 $\pm$ 1.5
	b	5002.60 $\pm$ 0.4	563 $\pm$ 27	18.0 $\pm$ 1.5
(Three components to model the H $\beta$ line)				
H $\beta$	n1	4862.6 $\pm$ 0.1	231 $\pm$ 21	1.4 $\pm$ 0.3
	n2	4858.6 $\pm$ 0.4	567 $\pm$ 25	1.9 $\pm$ 0.6
	b	4856.4 $\pm$ 1.2	2911 $\pm$ 210	18.9 $\pm$ 1.1
[O III] $\lambda$ 4959	n	4960.6 $\pm$ 0.1	231 $\pm$ 21	2.9 $\pm$ 0.4
	b	4956.5 $\pm$ 0.4	567 $\pm$ 25	6.2 $\pm$ 0.5
[O III] $\lambda$ 5007	n	5006.8 $\pm$ 0.1	231 $\pm$ 21	8.6 $\pm$ 1.2
	b	5002.6 $\pm$ 0.4	567 $\pm$ 27	18.5 $\pm$ 1.5
(Starlight contribution and three components to model the H $\beta$ line)				
H $\beta$	n1	4860.8 $\pm$ 0.5	307 $\pm$ 44	2.4 $\pm$ 2.6
	n2	4855.4 $\pm$ 0.7	408 $\pm$ 56	1.3 $\pm$ 2.7
	b	4856.7 $\pm$ 1.4	2657 $\pm$ 154	15.7 $\pm$ 3.3
[O III] $\lambda$ 4959	n	4958.8 $\pm$ 0.5	307 $\pm$ 44	5.6 $\pm$ 1.9
	b	4953.3 $\pm$ 0.7	408 $\pm$ 56	4.3 $\pm$ 1.2
[O III] $\lambda$ 5007	n	5006.8 $\pm$ 0.5	307 $\pm$ 44	16.8 $\pm$ 5.6
	b	5001.2 $\pm$ 0.7	408 $\pm$ 56	12.9 $\pm$ 3.7

Columns show: (1) emission line; (2) emission line components, where “n, n1, n2” and “b” represent the narrow and broad components, respectively; (3) the rest wavelength of the line component in angstroms; (4) FWHM of the line components (km s<sup>-1</sup>); (5) integrated line flux (10<sup>-16</sup> erg s<sup>-1</sup> cm<sup>-2</sup>).

& Lu 2001; Bian & Zhao 2004). We should use the line width of H $\beta$  coming from the BLRs to trace their virial movement. For SDSS J143030.22–001115.1, Williams et al. (2003) directly measured the width of the line halfway between the fitted continuum and the H $\beta$  line peak, and obtained an FWHM(H $\beta$ ) of 1744 km s<sup>-1</sup>. With this value in the empirical size-luminosity formula (Kaspi et al. 2000), we found its central supermassive black hole mass to be 10<sup>6.5</sup> M $_{\odot}$  and its Eddington ratio log L<sub>bol</sub>/L<sub>Edd</sub> to be -0.60 (Bian & Zhao 2004). Here we use the FWHM of the broad H $\beta$  to recalculate the black hole mass. Its mass would then be 0.44 larger if we take 2911 km s<sup>-1</sup> to be the FWHM(H $\beta$ ), or 0.41 larger if we take 2785 km s<sup>-1</sup>, and log L<sub>bol</sub>/L<sub>Edd</sub> would be -1.04  $\sim$  -1.01. If we use the FWHM of the narrow [O III] line to trace the bulge stellar velocity dispersion, then we find SDSS J143030.22–001115.1 to follow the so-called M<sub>bh</sub> -  $\sigma$  relation, M<sub>bh</sub> = 10<sup>8.13</sup> ( $\frac{\sigma}{200 \text{ km s}^{-1}}$ )<sup>4.02</sup> M $_{\odot}$  (Tremaine et al. 2002).

For seven NLS1s, Rodriguez-Ardila et al. (2000) found that the narrow component of H $\beta$  (H $\beta_n$ ) is about 50% of the total line flux and the [O III]  $\lambda$ 5007/H $\beta_n$  ratio emitted in the NLRs varies from 1 to 5, instead of the universally adopted value of 10. We also find the [O III] is not too weak in many SDSS NLS1s. This is consistent with the results of a sample of 64 NLS1s presented by Veron-Cetty et al. (2001). When we calculate the virial black hole masses of NLS1s, we should measure the H $\beta$  linewidth after subtracting the H $\beta$  contribution from NLRs, which is especially important for NLS1s with strong [O III] lines. For the mass correction of other objects in the sample of 150 NLS1s and their locus in M -  $\sigma$  plane, please refer to Bian, Yuan & Zhao (2006). The traditional definition of NLS1s by Osterbrock & Pogge (1985) and Goodrich (1998) does not consider multi-components in the H $\beta$  line. Therefore, we should be cautious about this

traditional definition and should consider using the BLR component of the  $H\beta$  line when classifying the NLS1s.

## 4.2 Starlight Contribution

The fibers in SDSS have a diameter of  $3''$  on the sky, corresponding to  $\sim 6.5$  kpc at the redshift of SDSS J143030.22–001115.1. Its SDSS spectrum taken through such a fixed aperture includes most of the emission from the host galaxy emission (petroRad<sub>r</sub> = 3.43''). At the same time, the nuclear luminosity is comparable with its host galaxy (psfMag<sub>r</sub> = 18.85 and petroMag<sub>r</sub> = 17.9). Using the method of Lu et al. (2006) (see also Li et al. 2005; Hao et al. 2005), the stellar component is modelled. The results are shown in Figure 3 and Table 3. The FWHM of the broad  $H\beta$  line is  $2657 \pm 154$  km s<sup>-1</sup>. Therefore, it is not a genuine NLS1 when we subtracted the  $H\beta$  contribution from the NLR.

## 4.3 X-ray Photon Index

ROSAT/ASCA X-ray observations of NLS1s showed that NLS1s generally have softer X-ray spectra than other AGNs, i.e., larger photon indexes  $\Gamma$ , where  $N_E \propto E^{-\Gamma}$  (e.g. Boller et al. 1996; Leighly 1999), but Williams et al. (2004) suggested that it is not always the case. They presented the Chandra observation of 17 NLS1s selected from the sample of 150 SDSS NLS1s (Williams et al. 2003), and derived  $\Gamma$  from spectral fitting in Sherpa or hardness ratio. They found two objects to have  $\Gamma$  less than one:  $0.25^{+0.80}_{-1.01}$  for SDSS J125943.59+010255.1,  $0.92 \pm 0.64$  for SDSS J143030.22–001115.1. For SDSS J125943.59+010255.1, its net Chandra 0.5–8 keV count rate is  $0.003 \pm 0.001$  and uncertainties of  $\Gamma$  are too large. For SDSS J143030.22–001115.1, as we have discussed above, it is not a genuine NLS1. We should remove these two objects when doing statistics of  $\Gamma$  of NLS1s. The mean  $\Gamma$  will be  $2.39 \pm 0.15$  and the standard deviation will be 0.59, when these two objects are excluded. Comparing with the result of Boller et al. (1996), the value of  $\Gamma$  is smaller, which is partially due to the different energy range coverage (Williams et al. 2004). It is suggested there is a correlation between  $\Gamma$  and the accretion Eddington ratio (e.g. Bian & Zhao 2003; Grupe 2004; Williams et al. 2004; Bian 2005). There possibly exist NLS1s with smaller Eddington ratios and flatter X-ray spectra.

It has been found that the optical properties of some NLS1s with flat X-ray spectra are not very different from those with steep X-ray spectra. The Eddington ratio of the former may be smaller than the latter. The NLS1s as presently defined are unlikely to be a homogeneous class. The apparent scarcity of ‘‘NLS1s’’ with low Eddington ratios should result in the following selection effect: in flux limited surveys, it is difficult to find AGNs with small black hole and low mass accretion rate.

**Acknowledgements** We thank Luis C. Ho for his very helpful comments. We thank Dr. H. Y. Zhou, for his useful remarks. This work has been supported by the NSFC (Nos. 10403005, 10473005 and 10273007) and the Science-Technology Key Foundation from Education Department of P. R. China (No. 206053). Funding for the creation and distribution of the SDSS Archive has been provided by the Alfred P. Sloan Foundation, the Participating Institutions, NASA, the National Science Foundation, the US Department of Energy, the Japanese Monbukagakusho, and the Max Planck Society. The SDSS Web site is <http://www.sdss.org/>. This research has made use of the NASA/IPAC Extragalactic Database, which is operated by the Jet Propulsion Laboratory at Caltech, under contract with NASA.

## References

- Abazajian K., et al., 2005, AJ, 129, 1755
- Bian W., Zhao, Y., 2003, MNRAS, 343, 164
- Bian W., Zhao, Y., 2004, MNRAS, 347, 607
- Bian W., 2005, ChJAA, 5(S), 289
- Bian W., Yuan Q., Zhao Y., 2005, MNRAS, 364, 187
- Bian W., Yuan Q., Zhao Y., 2006, MNRAS, 367, 860
- Boller Th., Brandt W. N., Fink H., 1996, A&A, 305, 53
- Goodrich R. W., 1989, ApJ, 342, 224

- Boroson T. A., Green R. F., 1992, *ApJS*, 80, 109  
Greene J. E., Ho L. C., 2005a, *ApJ*, 627, 721  
Greene J. E., Ho L. C., 2005b, *ApJ*, 630, 122  
Greene J. E., Ho L. C., 2006, *ApJ*, 641, L21  
Grupe D., Wills B.J., Wills D., Beuermann K., 1998, *A&A*, 333, 827  
Grupe D., Beuermann K., Mannheim K., Thomas H.-C., 1999, *A&A*, 350, 805  
Grupe D., et al., 2004, *AJ*, 127, 156  
Grupe D., 2004, *AJ*, 127, 1799  
Gu Q. S., et al., 2006, *MNRAS*, 366, 480  
Hao L., et al., 2005, *AJ*, 129, 1795  
Kaspi S., Smith P. S., Netzer H. et al., 2000, *ApJ*, 533, 631  
Kriss G. A., 1994, in: *ASP Conf. Ser. 61, Astronomical Data Analysis Software and Systems III*, eds. Crabtree D. R., Hanisch R. J., Barnes J., San Francisco: ASP, p.437  
Laor A., Fiore F., Elvis M. et al., 1997, *ApJ*, 477, 93  
Leighly K. M., 1999, *ApJS*, 125, 297  
Li C., et al., 2005, *AJ*, 129, 669  
Lu H., et al., 2006, *AJ*, 131, 790  
Mineshige S., Kawaguchi T., Takeuchi M. et al., Hayashida K., 2000, *PASJ*, 52, 499  
Osterbrock D.E., Pogge R., 1985, *ApJ*, 297, 166  
Pounds K. A., Done C., Osborne, 1995, *MNRAS*, 277, L5  
Rodriguez-Ardila A., et al., 2000, *ApJ*, 538, 581  
Stoughton C., et al., 2002, *AJ*, 123, 485  
Wandel A., Boller Th., 1998, *A&A*, 331, 884  
Wang T. G., Lu Y. J., 2001, *A&A*, 377, 52  
Williams R. J., Pogge R. W., Mathur S., 2003, *AJ*, 124, 3042  
Williams R. J., Mathur S., Pogge R. W., 2004, *ApJ*, 610, 737  
Tremaine S., et al., 2002, *ApJ*, 574, 740  
Veron-Cetty M.-P., Veron P., Goncalves A. C., 2001, *A&A*, 372, 730  
Zhou H. Y. et al., 2006, *ApJS*, in press (astro-ph/0603759)